First Clinical Experience Using Stereotactic Breast Biopsy Guided by ^{99m}Tc-Sestamibi

Angela Collarino[1,2]
Renato A. Valdés Olmos[1,3,4]
Peter A. Neijenhuis[5]
Wietske C. den Hartog[6]
Frederik Smit[1,3,7]
Lioe-Fee de Geus-Oei[1,2,8]
Lenka M. Pereira Arias-Bouda[1,7]

OBJECTIVE. The purpose of this study is to evaluate a new device using molecular breast imaging (MBI) for ^{99m}Tc-sestamibi–guided stereotactic lesion localization as a complementary biopsy tool.

MATERIALS AND METHODS. From December 2012 to May 2016, a total of 38 consecutive women (mean age, 59 years; range, 41–77 years) underwent ^{99m}Tc-sestamibi–guided biopsy using a new MBI-based device and were retrospectively reviewed. The biopsy modality used five steps: stereotactic localization of the ^{99m}Tc-sestamibi–avid lesion, calculation of coordinates of the lesion location using dedicated software, placement of the needle, verification of the correct needle position, and tissue sampling with a vacuum-assisted device followed by placement of a radiologic marker at the biopsy site and ex vivo measurement of the biopsy specimens.

RESULTS. The procedure was technically successful in all 38 lesions. In all cases, biopsy samples were radioactive and adequate for histopathologic analysis. Nineteen lesions (50%) were found to be malignant, and the remaining lesions were found to be benign. The mean procedure time was 71 minutes (range, 44–112 minutes). The radiologic marker was successfully deployed in 37 lesions (97%). Two hematomas and three vasovagal reactions were observed.

CONCLUSION. Technetium-99m sestamibi–guided biopsy performed using a dedicated MBI-based device is technically feasible and represents a valuable complementary biopsy tool in breast lesion diagnosis.

Keywords: ^{99m}Tc-sestamibi, breast cancer, molecular breast imaging, radioguided biopsy

DOI:10.2214/AJR.17.18083

Received February 13, 2017; accepted after revision May 28, 2017.

Based on a presentation at the European Association of Nuclear Medicine 2015 congress, Hamburg, Germany.

[1]Section of Nuclear Medicine, Department of Radiology, Leiden University Medical Center, Albinusdreef 2, 2333 ZA Leiden, The Netherlands. Address correspondence to L. M. Pereira Arias-Bouda (L.M.Pereira_Arias-Bouda@lumc.nl).

[2]Biomedical Photonic Imaging Group, MIRA Institute, University of Twente, Enschede, The Netherlands.

[3]Interventional Molecular Imaging Laboratory, Department of Radiology, Leiden University Medical Center, Leiden, The Netherlands.

[4]Department of Nuclear Medicine, The Netherlands Cancer Institute–Antoni van Leeuwenhoek Hospital, Amsterdam, The Netherlands.

[5]Department of Surgery, Alrijne Ziekenhuis, Leiderdorp, The Netherlands.

[6]Department of Pathology, Alrijne Ziekenhuis, Leiderdorp, The Netherlands.

[7]Department of Nuclear Medicine, Alrijne Ziekenhuis, The Netherlands.

[8]Department of Radiology and Nuclear Medicine, Radboud University Medical Centre, Nijmegen, The Netherlands.

AJR 2017; 209:1367–1373

0361–803X/17/2096–1367

Since 1994, technetium-99m–labeled sestamibi has been used as a tumor-seeking radiotracer to detect breast cancer [1, 2]. Uptake of ^{99m}Tc-sestamibi occurs within the mitochondria of tumor cells and is related to regional blood flow, angiogenesis, mitochondrial density, and activity [3–5]. Currently, ^{99m}Tc-sestamibi is the radiotracer of choice for molecular breast imaging (MBI). This modality, also called breast-specific gamma imaging, consists of a single- or dual-head small FOV gamma camera designed for breast imaging [6–10].

To date, MRI is the most commonly used imaging modality for breast cancer, after mammography and ultrasound (US). However, because of the limitations of MRI, such as high costs, limited use for patients with claustrophobia, obesity, or renal failure [11], and a high rate of unnecessary biopsies [12], MBI is evolving as a valuable complementary tool in the diagnostic workup of breast cancer [12, 13]. According to the Society of Nuclear Medicine and Medical Imaging, MBI is indicated as an adjunct imaging tool to mammography and US for the following patients: patients with newly diagnosed breast cancer for whom MBI is used to assess multifocal, multicentric, or contralateral disease; patients at high risk for BC; those with indeterminate breast lesions and remaining diagnostic concerns; and those with technically difficult breast imaging [14].

For patients with occult lesions on mammography and US that are ^{99m}Tc-sestamibi avid on MBI and are classified as BI-RADS category 4 or 5 [14, 15], second-look US is mandatory. If a sonographic substrate is found on second-look US, US-guided biopsy is performed during the clinical workup. However, for patients with suspicious MBI-detected lesions (BI-RADS category 4 or 5) that remain occult after second-look US or for patients with unclear lesions on mammography and US for whom mammography- or US-guided biopsy is considered technically impossible or has failed, other methods for accurate tissue sampling are necessary. Recently, a device for performing ^{99m}Tc-sestamibi–guided

Fig. 1—Molecular breast imaging–guided biopsy device equipped with compact stereotactic localization system containing fiducial source (*arrowhead*), grid paddle (*thin black arrow*), slant-hole collimators (*thick black arrow*), and detector (*white arrows*). Monitor displays breast images from two angles for calculation of *x*, *y*, and *z* coordinates of lesion and for determination of corresponding grid hole to insert needle.

breast biopsy with the use of dedicated MBI was developed. This tool is based on stereotactic localization of ^{99m}Tc-sestamibi–avid lesions with the use of a slant-hole collimator system and vacuum-assisted device [16, 17]. The purpose of the current study is to evaluate the potential of this device as a complementary biopsy tool.

Materials and Methods

Patients

From December 2012 to May 2016, a total of 38 consecutive patients (mean age, 59 years; range, 41–77 years) underwent ^{99m}Tc-sestamibi–guided biopsy using a dedicated MBI device. Before the procedure, two nuclear medicine physicians in consensus evaluated the MBI images and assessed the feasibility of performing MBI-guided biopsy. Clinical data were retrospectively reviewed. All patients gave written informed consent for retrospective analysis of the data, and the study was approved by institutional review board. All biopsied lesions were ^{99m}Tc-sestamibi avid on MBI (BI-RADS category 4 or 5) and were occult after second-look US or unclear on mammography and US without the possibility for mammography- and US-guided biopsy.

Technetium-99m–Labeled Sestamibi–Guided Biopsy Procedure

All biopsies were performed using ^{99m}Tc-sestamibi for radioguidance. A dedicated MBI device equipped with a stereotactic localization system (GammaLōc, Dilon Technologies), cleared by the U.S. Food and Drug Administration in 2009, was used to localize the target lesion (Fig. 1). The methodologic aspects of this MBI-based biopsy device have been described elsewhere [18]. All patients received analgesics for pain relief on the day of the procedure. After fixation of the breast between the detector and the compression paddle while the patient was in a seated position, a dose of 600 MBq of ^{99m}Tc-sestamibi was IV administered.

The biopsy procedure subsequently was performed in five steps. In step 1, a scout image was acquired, followed by acquisition of left and right stereotactic images to determine lesion location. In step 2, software for the dedicated MBI device equipped with a stereotactic localization system calculated the *x*, *y*, and *z* coordinates of the ^{99m}Tc-sestamibi–avid lesion location. In step 3, local anesthetic was injected and the needle was placed, and in step 4, verification of the correct needle position was performed using a ^{139}Ce source, as previously described and illustrated in detail elsewhere [18]. In step 5, biopsy was performed using a vacuum-assisted device. As a rule, six specimens were obtained. Immediately thereafter, a radiologic marker (clip) was placed at the biopsy site. After biopsy, the breast was removed from the detector. The radioactivity of the tissue samples was measured ex vivo with use of the MBI gamma camera to confirm the representativity of the biopsy specimens.

The biopsy samples were subsequently sent for histopathologic analysis. Breast mammography was performed immediately after the biopsy procedure to verify the correct position of the clip in all patients. For individual patients, further diagnostic steps were discussed during a multidisciplinary meeting attended by a radiologist, a nuclear medicine physician, a breast surgeon, and a pathologist. Subsequent decision making depended on such factors as histopathologic diagnosis, pretest likelihood for malignancy, activity of the acquired samples, and visibility of the index lesion on radiologic imaging.

If a patient with a malignant lesion was scheduled for breast-conserving surgery, the tumor was preoperatively localized using a wire or ^{125}I seed, which was placed at the site of the clip using sonographic guidance. For patients with benign histopathologic findings, the individual plan may vary from follow-up with MBI or MRI performed after 3–6 months (including resampling when indicated) to follow-up with mammography and US after 6–12 months or a return to the screening program (if applicable).

Data Collection and Analysis

Collected data included patient age, characteristics of the lesions based on ^{99m}Tc-sestamibi uptake according to the lexicon for MBI [15], clip placement, complications, and histopathologic findings after vacuum-assisted biopsy and surgical excision. The procedure time was determined by calculating the interval between initiation of acquisition of the scout image and placement of the clip at the biopsy site. The histopathologic findings from biopsy and excision were classified as follows: malignant lesions (invasive ductal carcinoma), invasive lobular carcinoma, ductal carcinoma in situ (DCIS), or a combination of these types of lesions; high-risk lesions such as atypical ductal hyperplasia (ADH) and lobular carcinoma in situ [19]; and benign lesions. Data were entered into a computerized spreadsheet (Microsoft Excel 2010) for analysis. Categoric variables were summarized as counts and percentages in each class. Quantitative variables, such as mean values and SDs, median values, and minimum and maximum values, were calculated.

Results

The results of this study are summarized in Table 1. MBI-based biopsy was technically successful for all 38 patients (38 lesions). For all patients, samples were radioactive and adequate for histopathologic analysis. The procedure was well tolerated by all patients. The mean procedure time was 71 minutes (range, 44–112 minutes). For three patients, the mean procedure time was longer than 89 minutes (SD, 1) because of low ^{99m}Tc-sestamibi avidity (patient 10), a patchy uptake pattern (patient 3) making localization more difficult, and incorrect switching of the slant-hole collimators (patient 8). The median size of the lesions was 14.5 mm (range, 5–60 mm). Of the 38 lesions, nine (24%) were located in the posterior third of the breast and therefore were close to the chest wall.

Histopathologic analysis of the biopsy specimens revealed that 19 lesions (50%) were malignant, with nine of these lesions identified as invasive ductal carcinoma, two as both invasive ductal carcinoma and DCIS,

TABLE 1: Summary of Results

Patient	Age (y)	Sestamibi Characteristic								Histopathologic Finding	
		Lesion Size (mm)	Uptake Pattern	Uptake Score[a]	Breast	Quadrant	Lesion Depth	Clip Failure	Complication	From Biopsy	From Excision
1	52	12	Focal	3	L	UIQ	C	—	—	IDC and DCIS	IDC and DCIS
2	62	10	Focal	3	R	UIQ	P	—	Hematoma	DCIS	DCIS
3	63	60	Patchy	2	R	UOQ	C	Migration	—	Mastopathy	
4	68	40	Focal	3	R	UOQ	C	Migration	—	DCIS	DCIS
5	56	7	Focal	2	L	LOQ	C	—	—	Mastopathy	
6	77	5	Focal	3	R	UIQ	C	—	—	IDC	IDC and DCIS
7	69	15	Focal	3	R	LOQ	P	Failed	—	Mastopathy	
8	55	25	Patchy	2	R	UOQ	C	—	—	Mastopathy and adenosis	
9	57	20	Focal	2	R	LOQ	P	—	—	IDC	IDC
10	53	30	Patchy	1	R	UOQ	C	—	—	Mastopathy	
11	72	11	Focal	2	R	UIQ	C	—	—	DCIS	No malignant focus
12	56	11	Focal	1	L	UIQ	C	—	—	ILC	ILC
13	75	10	Focal	3	R	UOQ	C	—	—	DCIS	DCIS
14	75	11	Focal	3	L	UOQ	P	—	Hematoma	IDC	IDC and DCIS
15	67	25	Patchy	2	R	C	C	—	—	DCIS	IDC and DCIS
16	56	9	Focal	2	R	LIQ	C	—	—	Mastopathy	
17	51	15	Patchy	2	L	LIQ	P	—	—	DCIS	DCIS
18	69	30	Focal	3	L	UOQ	C	—	—	IDC	IDC
19	51	20	Patchy	2	R	C	C	—	Vasovagal	Mastopathy	
20	41	20	Patchy	2	R	UOQ	P	—	—	IDC	IDC
21	61	14	Focal	2	L	C	A	—	—	Mastopathy	
22	50	20	Focal	2	R	UOQ	C	—	—	Adenosis	
23	56	7	Focal	1	L	UOQ	C	—	—	Mastopathy and adenosis	
24	67	45	Focal	3	R	UOQ	C	—	—	IDC and DCIS	IDC and DCIS
25	73	8	Focal	2	L	C	C	—	—	IDC	IDC and DCIS
26	57	20	Focal	2	L	C	C	Migration	—	Adenosis	
27	50	30	Patchy	3	R	UOQ	P	—	Vasovagal	Mucinous carcinoma	Mucinous carcinoma
28	66	11	Focal	3	R	LIQ	C	Migration	—	IDC	IDC and DCIS
29	67	20	Patchy	2	R	UOQ	A	—	—	Mastopathy	
30	51	9	Focal	2	L	UOQ	C	—	Vasovagal	Mastopathy	
31	48	7	Focal	1	L	UOQ	C	—	—	Adenosis	
32	50	15	Focal	3	L	UOQ	A	—	—	Mastopathy	
33	71	11	Focal	1	R	UOQ	C	—	—	Adenoma and mastopathy	
34	46	45	Patchy	2	L	UOQ	C	—	—	Adenosis	
35	51	12	Focal	1	L	UOQ	C	—	—	IDC	IDC and LCIS
36	48	11	Focal	2	L	LIQ	P	—	—	Mastopathy	
37	47	11	Focal	3	L	UOQ	P	—	—	IDC	IDC
38	54	35	Patchy	1	R	C	A	—	—	Mastopathy and adenosis	

Note—Dash denotes no clip failure or no complication. L = left, UIQ = upper inner quadrant, C = central, IDC = invasive ductal carcinoma, DCIS = ductal carcinoma in situ, R = right, P = posterior, UOQ = upper outer quadrant, LOQ = lower outer quadrant, ILC = invasive lobular carcinoma, LIQ = lower inner quadrant, A = anterior, LCIS = lobular carcinoma in situ.

[a]A score of 1 denotes mild uptake; 2, moderate uptake; and 3, marked uptake [12].

one as invasive lobular carcinoma, one as mucinous carcinoma, and six as DCIS (Figs. 2 and 3). On MBI, these 19 malignant lesions had a median size of 12 mm (range, 5–45 mm). Five patients underwent mastectomy. The remaining 14 patients underwent breast-conserving surgery, with wire localization used for 12 patients and ^{125}I seed localization used for two patients. Of these 14 patients, 13 (93%) had negative surgical margins, with a median margin of 4.5 mm (range, 2–12 mm). In one patient (patient 15), the surgical margins were positive because of an extension of extralesional DCIS. For 18 of 19 malignant lesions, subsequent surgical excision confirmed the diagnosis of cancer. For one patient (patient 11) who had DCIS diagnosed after vacuum-assisted biopsy, no in situ carcinoma or invasive carcinoma was found after surgical excision. The small area of DCIS (11 mm) probably had been completely excised during ^{99m}Tc-sestamibi–guided biopsy. No high-risk lesions were found on histopathologic analysis of the biopsy specimens.

Nineteen lesions (50%) were diagnosed as benign, with mastopathy diagnosed in 11, adenosis in four, and both mastopathy and adenosis in four (Fig. 4). On MBI, the median size of these benign lesions was 15 mm (range, 7–60 mm). Placement of a localizing clip was successful in 37 of 38 lesions (97%). In one patient (patient 7), the marker-needle dragged out the clip from the biopsy site when it was removed from the breast. Postbiopsy mammography showed correct position of the clip at the biopsy site in 33 of 37 patients (89%) and migration of the clip from the biopsy cavity in the remaining four patients. Complications were encountered in five patients (13%). In two patients, a hematoma developed but was resolved with compression. In another three patients, a vasovagal reaction occurred immediately after introduction of the trocar needle, but it was not necessary to abort the procedure.

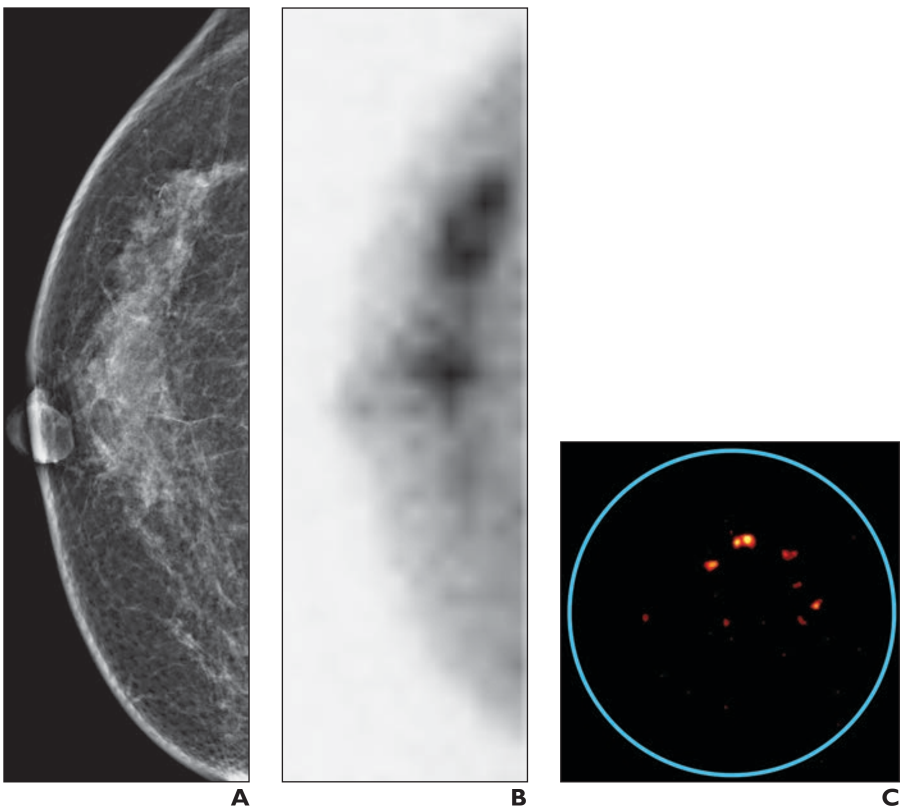

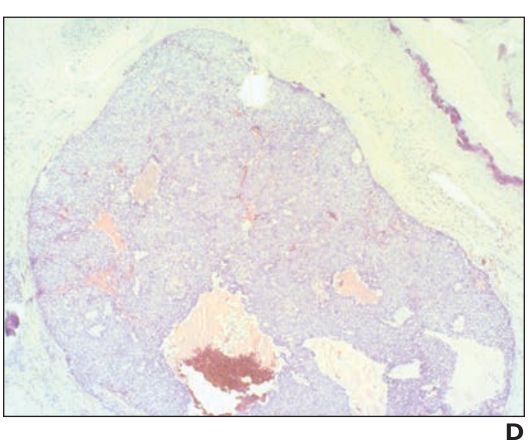

Fig. 2—68-year-old woman (patient 4) with ductal carcinoma in situ.
A, Right craniocaudal mammographic view shows no suspicious breast mass.
B, Right craniocaudal molecular breast imaging view shows two suspicious areas with focal ^{99m}Tc-sestamibi uptake in upper outer quadrant of small breast.
C, Scintigram of biopsy samples measured ex vivo shows radioactive specimens.
D, Composite photomicrograph (H and E, ×25) shows cancerization of lobule by intraluminal proliferation of atypical epithelial cells (ductal carcinoma in situ).

Discussion

In this first clinical experience with this new MBI-based device, ^{99m}Tc-sestamibi–guided biopsy was successful for all 38 consecutive patients. According to our results, this new biopsy tool appears to be technically feasible and may enable dedicated breast cancer imaging specialists to obtain radioactive samples from ^{99m}Tc-sestamibi–avid lesions on MBI. Furthermore, our results show that this device allows one to verify the success of the procedure by measuring ex vivo radioactivity in the biopsy specimens and to separate radioactive from inactive specimens, thereby enabling the pathologist to give special attention to the radioactive specimens (vital tissue), avoiding rebiopsy and delay in diagnosis.

According to our results, this biopsy procedure permits acquisition of adequate samples for histopathologic analysis because of the use of a vacuum-assisted device that obtains larger specimen volumes than does automated core needle biopsy [20, 21]. We have shown that ^{99m}Tc-sestamibi is useful in guiding the localization and excision of ^{99m}Tc-sestamibi–avid breast lesions. This potentially may facilitate the selection of the most ^{99m}Tc-sestamibi–avid areas that reflect the part of tumor with high cellular proliferation [22], leading to a more accurate genomic profile analysis [23] and avoiding sampling of stroma and fatty tissue, necrotic tissue, or both types of tissue, especially from large heterogeneous lesions. In our series, this new device allows successful sampling of subcentimeter lesions as well as lesions located in the posterior third of the breast and thus close to the chest wall. However, some posterior lesions may not be captured within the biopsy grid if they are in close proximity to the pectoral muscle, because they are not included in the FOV of the device [18].

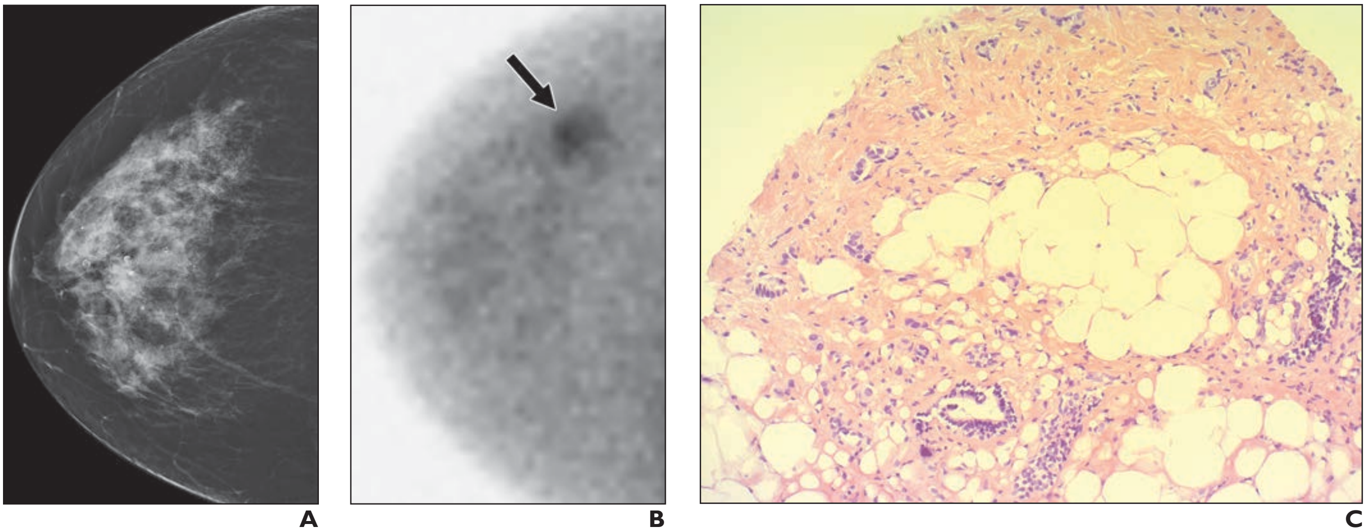

Fig. 3—57-year-old woman (patient 9) with invasive ductal carcinoma.
A, Right craniocaudal mammographic view shows no suspicious breast mass.
B, Right craniocaudal molecular breast imaging view shows one suspicious area with focal ^{99m}Tc-sestamibi uptake in lower outer quadrant of breast (*arrow*).
C, Composite photomicrograph (H and E, ×100) shows normal ductolobular units surrounded by irregular invasive glands and strands of atypical epithelial cells in stroma with desmoplastic changes and microcalcifications (invasive ductal carcinoma of no special type).

Placement of a clip at the biopsy site to facilitate subsequent excision, if needed, was successful in 97% of patients, a finding that is in concordance with findings from MRI-guided biopsies [24, 25]. In our series, the correct clip position was verified using mammography, which was performed immediately after biopsy, revealing a success rate of 89%, which is similar to data reported by Liberman et al. [24] for MRI-guided biopsy. Migration of the clip was encountered in four patients and was probably caused by the well-known accordion effect [26]. The time required for this new biopsy procedure appears to be comparable to that needed for MRI-guided biopsy [24, 27]. In the present study, time was principally spent acquiring the initial images necessary to localize the target lesion. The complications that were encountered are comparable to those reported in association with biopsy performed with MRI and a vacuum-assisted device [24, 25]. Hematoma can be controlled by postprocedural breast compression. Administration of antianxiolytic medication before the procedure could possibly reduce the number of vasovagal responses.

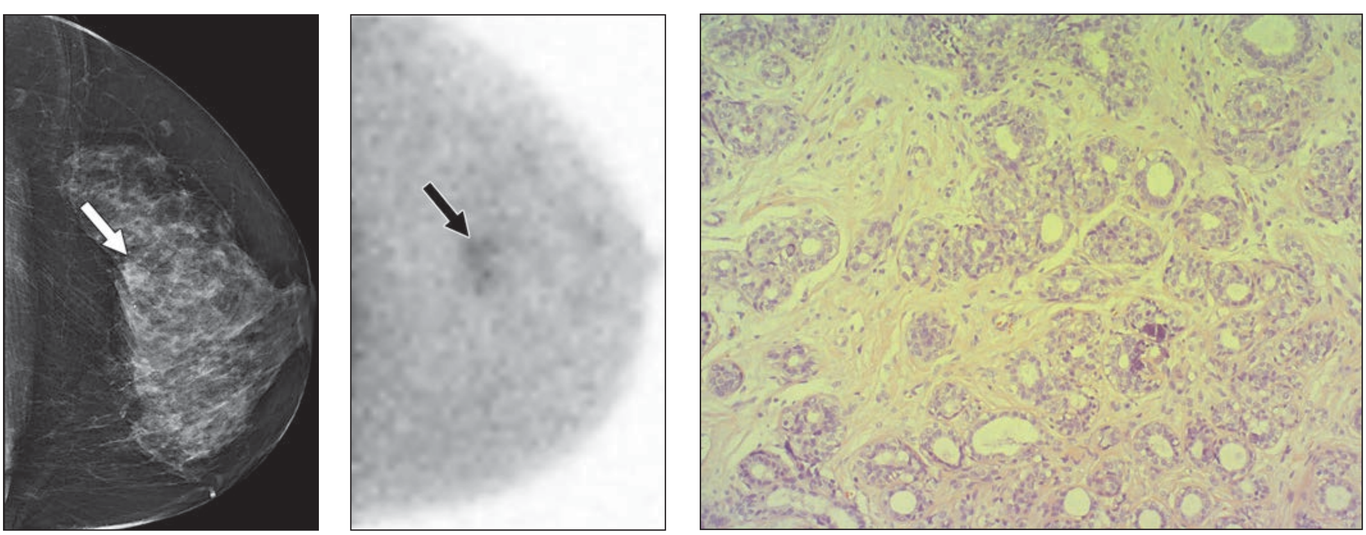

Fig. 4—57-year-old woman (patient 26) with adenosis.
A, Left craniocaudal mammographic view shows focally dense tissue (*arrow*) at central dorsal site of breast, which was considered to denote overprojection of normal fibroglandular tissue (probably benign; BI-RADS category 3).
B, Left craniocaudal molecular breast imaging view shows suspicious focal uptake of ^{99m}Tc-sestamibi (*arrow*) in center of breast, which is same area as BI-RADS category 3 lesion shown on mammographic view in **A**.
C, Composite photomicrograph (H and E, ×100) shows lobulocentric proliferation of mammary glands lined with two epithelial layers with glandular compression, distortion caused by stromal proliferation, and microcalcifications in lumina (adenosis).

This new biopsy device appears to be well tolerated by patients, is easy to use, and may cause less discomfort in patients with claustrophobia. In addition, it is not contraindicated in patients who are overweight or patients who have implanted devices or renal insufficiency. The relatively high percentage of malignancies found in our series emphasizes the value of this new biopsy tool at breast centers where MBI is implemented in the diagnostic pathway. Although half of the lesions biopsied because of MBI findings were found to be benign, this percentage is lower than the percentage of false-positive cases reported for MRI-guided biopsy [24]. MBI cases with false-positive results are the result of uptake of ^{99m}Tc-sestamibi in benign conditions such as adenosis and mastopathy.

The present study has limitations. First, the study is retrospective. Second, the population is relatively small, with a low enrollment rate; however, only patients with occult or unclear lesions for which the possibility of mammography- and US-guided biopsy was excluded were eligible. Third, the possible limitations of this modality are related to difficult localization of the lesion because of low or patchy uptake of ^{99m}Tc-sestamibi or localization of the lesion in close proximity to the thoracic wall. Furthermore, as with any other biopsy procedure, the possibility of sampling error should be considered in case of discordance between imaging features and histologic results. In this regard, an advantage of MBI-based biopsy over MRI-guided biopsy is the possibility of verifying ex vivo whether lesion sampling is successful by measuring the radioactivity in the samples. For discordant cases, further management will be accorded by the institutional multidisciplinary oncology committee and will depend on the initial level of suspicion on MBI, the radioactivity of the obtained biopsy samples, and visibility of or suspicion for the index lesion on mammography, second-look US, or both. If follow-up is requested, short-term (3-month) follow-up with MBI may be performed or follow-up with MRI may be done after 6 months to avoid imaging of postbiopsy tissue changes.

Another important aspect concerns the clip placed after biopsy. The fact that the clip is not visible on MBI may theoretically hinder verification of the correct position of the clip. In our experience, comparison of craniocaudal and lateromedial views from MBI with the corresponding views from postbiopsy mammography helps to solve this limitation because clip position can be adequately judged visually. In the future, coregistration in the acquisition of MBI and mammography images, followed by fusion of images, might help improve the procedure. Clip migration, however, may hamper preoperative lesion localization when the lesion is found to be malignant and is radiologically occult.

Finally, this procedure involves IV injection of a radioactive tracer and, thus, the use of ionizing radiation. Although the mean glandular dose to the breast is lower with MBI than with digital mammography, the estimated whole-body effective dose is 5 mSv with MBI (using 600 MBq of ^{99m}Tc-sestamibi), compared with 0.5 mSv with digital mammography and 1.2 mSv with mammography combined with digital breast tomosynthesis [28]. A single MBI study with 740–1110 MBq of ^{99m}Tc-sestamibi is associated with a lifetime attributable risk of fatal cancer that is 20–30 times greater than that of digital mammography in women aged 40 years [29]. One should notice that doses from both mammography and MBI are much lower than doses at which consideration of risks from radiation are warranted [30]. In addition, innovations in MBI technology allow a reduction in administered activity to 150 MBq of ^{99m}Tc-sestamibi, leading to significant reductions in the absorbed dose to the breast (0.25 mGy) and the effective dose (1.1 mSv) [28]. The fact remains, however, that one should strive to follow the as low as reasonably achievable (ALARA) principle for minimizing radiation exposure for each individual patient. In this context, the decision to perform MBI in the follow-up of patients with discordant pathologic findings or mistargeting during MBI-guided biopsy needs to outweigh the pros and cons based on patient characteristics, local options, and expertise. The introduction of modern MBI devices, working with lower administered radioactivity and reduced effective whole-body doses comparable to those delivered by digital mammography, may help to solve this limitation in the future.

In conclusion, ^{99m}Tc-sestamibi–guided biopsy using a dedicated MBI device is technically feasible and seems to represent a reliable complementary biopsy tool. Further studies with larger series of patients are needed to establish the definitive clinical relevance of this device.

References

1. Khalkhali I, Mena I, Jouanne E, et al. Prone scintimammography in patients with suspicion of carcinoma of the breast. *J Am Coll Surg* 1994; 178:491–497
2. Kao CH, Wang SJ, Liu TJ. The use of technetium-99m methoxyisobutylisonitrile breast scintigraphy to evaluate palpable breast masses. *Eur J Nucl Med* 1994; 21:432–436
3. Mankoff DA, Dunnwald LK, Gralow JR, et al. [Tc-99m]-sestamibi uptake and washout in locally advanced breast cancer are correlated with tumor blood flow. *Nucl Med Biol* 2002; 29:719–727
4. Scopinaro F, Schillaci O, Scarpini M, et al. Technetium-99m sestamibi: an indicator of breast cancer invasiveness. *Eur J Nucl Med* 1994; 21:984–987
5. Delmon-Moingeon LI, Piwnica-Worms D, Van den Abbeele AD, Holman BL, Davison A, Jones AG. Uptake of the cation hexakis(2-methoxyisobutylisonitrile)-technetium-99m by human carcinoma cell lines in vitro. *Cancer Res* 1990; 50:2198–2202
6. Brem RF, Schoonjans JM, Kieper DA, Majewski S, Goodman S, Civelek C. High-resolution scintimammography: a pilot study. *J Nucl Med* 2002; 43:909–915
7. Rhodes DJ, O'Connor MK, Phillips SW, Smith RL, Collins DA. Molecular breast imaging: a new technique using technetium Tc 99m scintimammography to detect small tumors of the breast. *Mayo Clin Proc* 2005; 80:24–30
8. Jones EA, Phan TD, Blanchard DA, Miley A. Breast-specific gamma-imaging: molecular imaging of the breast using ^{99m}Tc-sestamibi and a small-field-of-view gamma-camera. *J Nucl Med Technol* 2009; 37:201–205
9. Weinmann AL, Hruska CB, O'Connor MK. Design of optimal collimation for dedicated molecular breast imaging systems. *Med Phys* 2009; 36:845–856
10. Hruska CB, Weinmann AL, Tello Skjerseth CM, et al. Proof of concept for low-dose molecular breast imaging with a dual-head CZT gamma camera. Part II. Evaluation in patients. *Med Phys* 2012; 39:3476–3483
11. Berg WA, Blume JD, Adams AM, et al. Reasons women at elevated risk of breast cancer refuse breast MR imaging screening: ACRIN 6666. *Radiology* 2010; 254:79–87
12. Johnson N, Sorenson L, Bennetts L, et al. Breast-specific gamma imaging is a cost effective and efficacious imaging modality when compared with MRI. *Am J Surg* 2014; 207:698–701
13. Sun Y, Wei W, Yang HW, Liu JL. Clinical usefulness of breast-specific gamma imaging as an adjunct modality to mammography for diagnosis of breast cancer: a systemic review and meta-analysis. *Eur J Nucl Med Mol Imaging* 2013; 40:450–463
14. Goldsmith SJ, Parsons W, Guiberteau MJ, et al. SNM practice guideline for breast scintigraphy with breast-specific γ-cameras 1.0. *J Nucl Med Technol* 2010; 38:219–224

15. Conners AL, Hruska CB, Tortorelli CL, et al. Lexicon for standardized interpretation of gamma camera molecular breast imaging: observer agreement and diagnostic accuracy. *Eur J Nucl Med Mol Imaging* 2012; 39:971–982
16. Moadel RM. Breast cancer imaging devices. *Semin Nucl Med* 2011; 41:229–241
17. Weinmann AL, Hruska CB, Conners AL, O'Connor MK. Collimator design for a dedicated molecular breast imaging-guided biopsy system: proof-of-concept. *Med Phys* 2013; 40:012503
18. Collarino A, Valdés Olmos RA, van der Hoeven AF, Pereira Arias-Bouda LM. Methodological aspects of ^{99m}Tc-sestamibi guided biopsy in breast cancer. *Clin Transl Imaging* 2016; 4:367–376
19. Sewell CW. Pathology of high-risk breast lesions and ductal carcinoma in situ. *Radiol Clin North Am* 2004; 42:821–830
20. Liberman L. Centennial dissertation: percutaneous imaging-guided core breast biopsy—state of the art at the millennium. *AJR* 2000; 174:1191–1199
21. Berg WA, Krebs TL, Campassi C, Magder LS, Sun CC. Evaluation of 14- and 11-gauge directional, vacuum-assisted biopsy probes and 14-gauge biopsy guns in a breast parenchymal model. *Radiology* 1997; 205:203–208
22. Del Vecchio S, Salvatore M. ^{99m}Tc-MIBI in the evaluation of breast cancer biology. *Eur J Nucl Med Mol Imaging* 2004; 31:S88–S96
23. de Snoo F, Bender R, Glas A, Rutgers E. Gene expression profiling: decoding breast cancer. *Surg Oncol* 2009; 18:366–378
24. Liberman L, Morris EA, Dershaw DD, Thornton CM, Van Zee KJ, Tan LK. Fast MRI-guided vacuum-assisted breast biopsy: initial experience. *AJR* 2003; 181:1283–1293
25. Liberman L, Bracero N, Morris E, Thornton C, Dershaw DD. MRI-guided 9-gauge vacuum-assisted breast biopsy: initial clinical experience. *AJR* 2005; 185:183–193
26. Esserman LE, Cura MA, DaCosta D. Recognizing pitfalls in early and late migration of clip markers after imaging-guided directional vacuum-assisted biopsy. *RadioGraphics* 2004; 24:147–156
27. Perlet C, Heinig A, Prat X, et al. Multicenter study for the evaluation of a dedicated biopsy device for MR-guided vacuum biopsy of the breast. *Eur Radiol* 2002; 12:1463–1470
28. O'Connor MK. Molecular breast imaging: an emerging modality for breast cancer screening. *Breast Cancer Manag* 2015; 4:33–40
29. Hendrick RE. Radiation doses and cancer risks from breast imaging studies. *Radiology* 2010; 257:246–253
30. Hruska CB. Molecular breast imaging for screening in dense breasts: state of the art and future directions. *AJR* 2017; 208:275–283